Analysis of the Micro-type Circular Rod Screw Thread Machining Process

Tsung-Chia Chen
National Chin-Yi University of Technology
Hao-Wei Ting
National Chin-Yi University of Technology
Cheng-Chi Wang (wcc@ncut.edu.tw)
National Chin-Yi University of Technology https://orcid.org/0000-0002-3009-6571

Research Article

Keywords: Micro-type circular rod, Stainless steel, Finite element, Screw Thread

Posted Date: May 4th, 2021

DOI: https://doi.org/10.21203/rs.3.rs-454547/v1

Analysis of the Micro-type Circular Rod Screw Thread Machining Process

Tsung-Chia Chen[1], Hao-Wei Ting[1], Cheng-Chi Wang[2*]

[1]Department of Mechanical Engineering, National Chin-Yi University of Technology, Taichung 41170, Taiwan.

[2]Graduate Institute of Precision Manufacturing, National Chin-Yi University of Technology, Taichung 41170, Taiwan.

*Corresponding author:wcc@ncut.edu.tw

Abstract

The main purpose of this research is to study the analysis of the screw thread machining process for micro-type circular rods. During the analysis, the SUS304 stainless steel micro-type circular rod is used to analyze the micro thread machining process for the circular rod that will be fabricated according to varied outer diameters (Ø1.9mm, Ø1.94mm and Ø2mm), varied pitches (0.25mm and 0.4mm), and specific friction factors (0.1, 0.2, 0.3, 0.5 and 0.7). Through the micro material parameters with scale factors being corrected, the finite element analysis is conducted in order to learn about the effect of pitches and friction factors on the screw threads of the micro-type circular rod during the machining process. During the research, the finite element analysis was also conducted through the use of full integration rule and by coupling the shape function, as being inferred from the 3D tetrahedral element with 4 corner nodes, in the stiffness matrix. This research focuses on the simulation of comprehensive forming resume data, stress/strain distribution and thread shape distribution relating to the thread machining process for the micro-type circular rod. In the meantime, the micro-type circular rod screw thread machining die is also designed for carrying out the micro-type thread machining experiment for the SUS304 micro-type circular rod. The outcome is also compared with the simulation result to verify the reliability of the aforesaid analysis method. During the research, the difference between traditional material parameters and that of the corrected micro dimensions is also analyzed with the result provided below: The simulation result of the corrected material parameters indicated that the maximum principal stress tends to grow along with the enlarging of the pitch, but there isn't a visible difference between the maximum principal strain and the material parameters being used before and after the modification. When the friction factors are changing during the micro-type circular rod screw thread machining process, its torsional, stress, and strain force tends to grow along with the increase of friction factors.

Keywords： Micro-type circular rod, Stainless steel, Finite element, Screw Thread

1. Introduction

With the miniaturization trend progressing in the manufacturing realm, the demand for micro-type parts is becoming bigger. When the 80's in the 20th century emerged, the traditional plasticity machining process was applied in the micro-forming techniques required for manufacturing a massive amount of micro-forming metal components. Nowadays, such a new-rising technique has been widely used in the miniaturization tide for manufacturing cell phones and medical, mechanical, and digital products. As the micro-forming technique is featuring on faster manufacturing speed and lower cost advantages, it is especially suitable for a massive amount of production. It is, therefore, a very important technique for the subtle type of manufacturing. Its technical cores shall mainly include the materials, die, inspection/testing and environment. With the evolution of time over the past years, slimmer, shorter, lighter and more compact products have now become the mainstream, and the fasteners required for these devices are also changing along with the tide. By using the thread-forming fasteners, it not only eliminates the tedious striking and tapping steps but also saves the expensive built-in mounting pieces that will be required before and after the forming process.

The historical literature prepared for the metal forming indicated that the 3D finite element analysis theory was employed by Makinouchi and Kawka[1] in 1994 to study the design using the finite element to simulate the stampling die. During the research, the value simulation analysis was conducted to estimate the issues that may result in the defects during the metal stampling process to replace the traditional "trial and error" method, hoping to reduce the error probability and increase the production speed for the product. In 2002, Engel[2] et.al. proposed the Sub-millimeter machining process upholding that the size of two parts being produced during the metal forming will be smaller than 1mm. It is called the Micro Metal Forming theory. Because the micro forming process will be affected by the dimensional effect, apart from reducing the forming load, it will also affect relevant phenomena such as the surface coarseness of the component, the friction force during the forming process, the flow stress of the material and the

bouncing effect, etc. In 2010, Peng et.al. [3] studied the evolution of friction behavior from micro dimensions to macro dimensions and then proposed an innovative uniform friction model based on the hypothetic open/close lubricant bag theory. By using the newly developed friction model, they conducted the Finite Element (FE) Simulation in order to analyze the friction dimensional effect during the ring compression process and the result indicated that the radial friction force is totally different from the inner diameter and outer diameter as far as the changing is concerned; therefore, its tendency is exactly consistent with the experiment result. In 2013, Ryoichi Chiba [4] proposed a probabilistic method that can be used to estimate the reliability regarding the forming limit of the anisotropic metal plate provided with uncertain material properties in order to study the influence of uncertain material properties on the forming limit curve and the resulting strength.

The literature prepared for the screw thread forming analysis explained the influence of the machining parameters being selected by Joseph P. Domblesky and Feng Feng [5] in 2002 on the material flowing and the thread profile of the large-diameter blank during the external thread rolling process. During the research, they discovered that the Plane Strain Model provide reasonable proximity during the thread rolling process. It has changed the influence to the effective strain and the thread height that will be posed by the thread type, friction coefficient flow stress and blank diameter. The FM software being used is called “DEFORM” software. In the meantime, U. Engel and R. Eckstein[6] studied the miniaturization-related issues to develop the fundamental research initiated solutions and display the result of micro-forming progress. In 2004, Z. Pater, A. Gontarz and W. Weroñski[7] proposed the research and execution method that can be completed within the frame of the thread rolling techniques being newly developed for the concrete tie securing screws. Concerning this, the thread rolling method comprises the thread forming for two pieces of wedge-shaped parts that are provided with a special groove required for executing the thread forming. Further, they also proposed the result of theoretical and experimental research related to the forming of new screws. The practical screw forming process comprises the screw head flash forging and the thread rolling. The innovative machining method being proposed also includes the flash-free forging and thread forming as well as the use of the cross-wedge rolling technique in dual-type configuration [8]. In 2006, Kao et. al.[9] studied the research on the integrated CAD/CAE/CAM system that will be used to form the geometrical structure for the thread-rolling die. During the research, they selected an industrial proven case to verify the integrated CAD/CAE/CAM process. The result revealed a very inspiring finding that it had demonstrated the feasibility of using such a system in industrial applications. In 2011, Kai-Neng Hwang [10] studied the influence of magnesium alloy LZ91 mini screw tapper and thread milling process related parameters on the forging force and the metal flowing type; in the meantime, they also conducted the formability analysis and the process parameter analysis by using DEFORM-2D software to simulate mini-size screw tapper and the thread rolling techniques. In 2014, Yung-Chin Li[11] studied the effect of micro thread tapping on a thin stainless steel plate (SUS304) in order to analyze the thread tapping quality according to the thread tapping torque and the post-rolling area size. By comparison, the Taguchi Method can be used to study the parameters of a certain quality and it cannot solve the issues resulting from multi-quality parameters. For this reason, the Grey Relational Theory is based on obtaining the optimal parameters for multi-quality processes in order to achieve the ultimate effect for the micro-thread tapping tool.

Aiming at the sudden breaking problem of the threads when tapping the mini-diameter internal threads of the titanium alloy, Swapnil Pawar and Suhas S. Joshi[12] proposed a comprehensive experiment in 2016 to study the tapping mechanism and performance of the Axial Vibrating Auxiliary Tapping (AVAT) and Axial Torsional Vibrating Auxiliary Tapping (ATVAT) that will be applied to the titanium alloy. They discovered that without affecting the thread mass, the AVAT and ATVAT can reduce the tapping torque, axial force, and temperature that traditional tapping cannot achieve (CT). The micro-structure of the tapping surface reveals that the area affected by the ATVAT and the AVAT type of tapping method is less than that by the CT method. Aiming to the problem where the development of traditional tapping tool is usually composed by the expensive investigation and experiment, a method was proposed by Ekrem Oezkaya and Dirk Biermann[13] in 2017 upholding that such method can be used during the design stage to estimate the relative torque so as to save the resources, energy and cost. Based on the referential simulation model that accords with the experiment result, the lengthy calculation time issue can be solved through the appropriate segmentation method. As such, total load circulation can be concluded through a corresponding mathematical model and discontinued torsional curve.

In this article, the metric system thread is based to set up the micro-type circular rod screw thread machining process. The area that is mostly affected by the process parameters is the tooth root of the micro-type circular road threads and where the thinnest thickness exists. Therefore, it is very important to the screw die design. During the research, the thread machining process is analyzed for the micro-type circular rod with different pitches. In the meantime, the simulation analysis is also conducted according to the circular rods presenting varied diameter and thickness as well as varied friction factors. The factory will use the result to use as a

reference for a die design to minimize unnecessary "trial-and-error" procedures during the operation process in order that a reliable analysis mode will be available to improve the productivity and to fortify the competitiveness.

2. Analysis Method

2.1 Simulation Analysis

The metallic plate selected for this research is made of SUS304 stainless steel. In this regard, the stainless steel belongs to the BBC crystalized structure provided with special chemical and physical characteristics and it is one of the corrosion-resistant alloy materials normally used by the industrial and medical industries. The article will be focusing on the elastoplastic deformation with the following hypothesis provided in the meantime:

1. The screw die and lower die are assumed as the rigid body.
2. Assuming that all materials are presenting homogeneous properties.
3. The elasticity and plasticity strain rate is considered for the strain rate of the material.
4. The temperature influence and the existence of internal stress will not be considered during the forming process.
5. The materials shall be treated according to the yielding conditions proposed by von Mises, and the plastic flow rule proposed by Prandtl-Reuss shall be followed after the plasticity deformation.

In this article, the simulation is conducted with the DEFORM-3D finite element analysis software by considering the screw die as the rigid body and the micro-type circular rod as the plastic body and all materials are assumed as under homogeneous and isotropic conditions. Indicated in Fig. 1 is the action method of the screw die and the micro-type circular rod. The screw die tends to engage with the circular rod's surface during the circular rod thread machining process, and the nodes that are contacting or detaching from the screw die must be clearly defined. The node shall be divided into contact nodes and free nodes. The node not contacting the die will be defined as free node for which the all area space coordinate (X, Y or Z) shall be used. The node contacting the die will be defined with a local coordinate (ξ, η, ζ) according to the right-hand rule at that time.

By employing the formula composed by the Update Lagrangian Formulation (ULF) Theory relating to the finite deformation and the scale factor modified materials, one will be able to infer the governing equation that will be suitable for the machining process for all types of metals step by step.

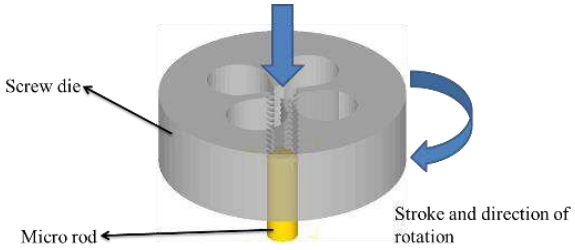

Fig. 1 Action Method of Screw Die and Micro-type Circular Rod

When executing the thread tapping simulation with DEFORM-3D, the number of grids will affect the outline of the tapping. The more the number of grids, the longer time will be required for analytical computation and the data to be stored for analytical computation will also become enormous. To achieve a more efficient simulation of thread tapping, normally, the number of the grids will be set at 60000 for carrying out the simulation. Indicated in Table 1 are the simulation parameters.

Table 1 Simulation Parameters

Material	SUS304
Dimensions of material (mm)	6
Friction Factor (m)	0.1, 0.2, 0.3, 0.5, 0.7
Pitch (mm)	0.25, 0.4
Number of Grid	60000

In the meantime, the "plastic flow rule" proposed by Prandtl-Reuss and the yielding conditions proposed by Hill are also selected. Regarding yielding condition judgment, the yielding conditions proposed by von Mises are especially used with Hill's proposed. The yielding conditions proposed by von Mises are used in the isotropic materials and those proposed by Hill are used in introducing the anisotropic parameters with anisotropic materials considered accordingly. In the meantime, the finite element deformation theory and the ULF concept are also combined for creating an increment type of elastoplastic deformation finite element analysis mode. Further, the shape function inferred from the tetrahedral element with 4 corner nodes is also employed for coupling to the stiffness matrix in order to form the Finite Element Analysis Mode. Furthermore, the Full Integration Rule calculation method is also employed to infer the stiffness matrix relating to the tetrahedral element with 4 corner nodes. When dealing with the friction issue between the screw die and the blank, the modified Coulomb Friction Law is selected. In this respect, the modified Coulomb Friction Law can be used to deal with the friction of the contacting face that is under a discontinued sliding-sticking condition in order

to maintain the linear increment computation. In the meantime, the dimensional effect resulting from miniaturization is also considered in order to modify the traditional material model with the scale factor modification formula for the convenience of studying the computer-aided works. In this way, the software shall be able to display the forming diagram and the stress/strain distribution diagram. It can also display the relationship between the torque and the stroke according to the change resulting from the pitches, friction factors and circular rod diameter, and displaying the distribution status of max. principal stress and max. principal strain.

2.2 Scale factor relating to dimensional effect

As affected by the dimensional effect, significant errors were found between Finite Element Analysis and actual product during the micro-forming process that the traditional material model cannot be used. For this reason, a new material model should be developed by considering the dimensional effect. In this Plan, the SUS304 is used to carry out the Tensile Strength Test to study the influence of dimensional effect on the micro-type circular rod. In the meantime, a new micro elastoplastic material model is also developed to compare its difference with the traditional material model. Therefore, the stress-strain formula between the circular rod and the traditional macro-based material is modified here by the proportional method without considering the material's dimensional effect. As such, the Swift material model is adopted as follows:

$$\overline{\sigma} = K\left(\varepsilon_o + \overline{\varepsilon_p}\right)^n \quad (1)$$

where, σ and ε represent true stress and true strain respectively; whereas, K and n represent the material constant.

In this research, the circular rod diameter "d" is used as the scale factor for modification. According to the true stress and the true strain diagram obtained from the tensile strength test, the traditional material model should be used if the circular rod diameter is over 2.2.mm; whereas, the modified material model should be used if the circular rod diameter is less than 2.2.mm. When using the diameter of a micro-type circular rod as the modifying factor, because the circular rod diameter being selected for this research is 2mm, the traditional material model is modified by proportional methods according to the stress-strain formula established for calculating traditional materials in Eq.(2), as provided below:

$$\overline{\sigma}(d,\overline{\varepsilon}) = fMe^{gd}(\varepsilon_0 + \overline{\varepsilon_p})^{n(he^{id}-1)} \quad (2)$$

Where, "f, g, h and I" represent the proportional values being modified, and "d" refers to the circular rod diameter. In the research conducted by F. Liu, the result indicated that the modifying value [14] contained in the aforesaid formula can be effectively resolved with the least square method, as per the structure in Eq. (3). Based on the stress-strain relationship obtained in the previous tensile strength test, the values are selected from 10 data pointss for each individual diameter to carry out the calculation. Therefore, the formula is revised as that indicated in Eq. (4).

$$\min_{X\in R^n} f(x) = \frac{1}{2}\left\|F(x)\right\|_2^2 = \frac{1}{2}\sum_t F_i(x)^2 \quad (3)$$

$$\min f(f,g,h,i) = \frac{1}{2}\sum_d\sum_{j=1}^{10}(\overline{\sigma}_j - \sigma_k F_j(d,\overline{\varepsilon}_j))^2 \quad (4)$$

To calculate the optimal value for "f (f, g, h, i)", the Levenberg-Marquart Method is used in this research in order to search such value. Such a method is established by combining the advantages of Newton Law and the Steepest-descent Method. As the search direction selected for the early-stage iteration process is closer to the gradient direction, it is approximate to the Steepest-descent Method; whereas, the later-stage iteration is approximate to the direction provided by the Newton Law. With the aforesaid method, minimal value is therefore acquired for "f, g, h and I" respectively, as per Table 2.

Table 2. Proportional Value for Modification Formula

f	g	h	i
0.7364	0.3165	1.0112	-0.01032

By substituting the proportional values in Eq.(2), the modified formula is provided in Eq.(5)as below:

$$\overline{\sigma}(d,\overline{\varepsilon}) = 0.7364Me^{0.3165d}(\varepsilon_0 + \overline{\varepsilon_p})^{n(1.0112e^{-0.01032d}-1)} \quad (5)$$

Because this article is using the material model with the diameter of a circular rod is set at 2mm for carrying out the modification of proportional value, the "M, n" values in Eq. (5) should be substituted by using the data obtained from the circular rod with the diameter being set at 2mm in which, "M" value represents the "K" value in such parameter and the values obtained for the stainless steel are 1819Mpa and 0.576 respectively. As such, indicated in Eq. (6) is the final material model for which the diameter has been modified.

$$\overline{\sigma} = 1340e^{(0.3165d)}(0.077 + \overline{\varepsilon_p})^{0.5824e^{(-0.01032d)}-1} \quad (6)$$

2.3 Tensile Strength Test

In this experiment, the stainless steel micro-type circular rod is made of SUS304 and the material parameters are indicated in Table 3. In the meantime, its values are the parameters obtained after modifying the scale factors:

Table 3. Mechanical Properties and Material Parameters for SUS304 Stainless Steel

Material	E(GPa)	v	σ_y(MPa)
SUS304	207	0.3	316
K(MPa)	n	ε_0	K(MPa)
2518.5	0.576	0.077	2518.5

Where, E: Elastic Coefficient; v: Posson's Ratio; σy: Yielding Stress

During the experiment, the Tensile Strength Test has been conducted for the 2.0mm micro-type circular rod with the Micro-computer Tension Tester and the load range is below 200kg. Because the chuck of this machine cannot clamp the micro-type circular rod securely, another set of chuck is added in the testing machine together with another two sets of hand-held chucks to clamp the micro-type circular rod in position. The tensile strength test is a kind of convenient testing method being widely used. Lots of basic mechanical properties can be acquired when the material is subjecting to strengthening axial load during the test. During the test, the stress-strain curve is observed in order to analyze the properties relating to the material, such as the level of tensile strength and the elasticity limit, etc. In view that the length and the diameter of the tested material (i.e. micro-type circular rod) are too small that it cannot be held in position easily and the size of the Test Piece is also beyond the specifications established for the Standard Test Piece, therefore markings are made at 10mm from both ends of the micro-type circular rod for using the stretching positions. By doing so, the chucks required for the machining are secured to the upper and lower chuck positions of the stretching machine by the screw fastening method and then lock the micro-type circular rod in position with the hand-held chuck. As a next step, the machine stretching speed is set at 2mm/mm for carrying out 3 rounds of tensile strength test for the micro-type circular rod for obtaining the desired stretching value, respectively, whichever is the greatest. After that, such value is translated to the stress-strain diagram in order to proceed with the analysis.

Based on Eqs. (7) and (8), the engineering stress (s) and the engineering strain (e) obtained from the Tensile Strength Test are then translated to true stress (σ) and true strain (ε) respectively.

$$\sigma = \frac{F}{A} = s(1+e) \tag{7}$$

$$\varepsilon = \ln(\frac{L}{L_o}) = \ln(1+e) \tag{8}$$

Where $S = F/A_o$ (engineering stress), $e = \Delta L/L_o$ (engineering strain)

The relationship between true stress and true strain can be described with the Eq.(1) for which the K and n values are obtained according to the least root-mean-square method. The result indicated that the plastic flow stress would present visible change along with the fluctuation of micro-type circular rod diameter. The bigger the micro-type circular rod diameter, the higher the material's plastic flow stress. This is mainly due to the shrinking of the Test Piece diameter that has reduced the crystal grains on the cross-sectional profile of the Test Piece. The Tensile Strength Test proves that a significant dimensional effect will exist when judged from the micro-scale point of view.

2.4 Analytical steps

The analysis procedure includes 9 steps shown in Fig. 2 and as following:

1. Conduct the Tensile Strength Test to study the impact of the dimensional effect.
2. Conduct the Elastoplastic Deformation FE Analysis and use the DEFORM analysis program.
3. Design the 3D model for the die and the blank.
4. Conduct the Finite Element Simulation Analysis and check if any defect is presented during the forming process. If any defect exists, then the product and the die required for the forming must be designed again.
5. Start fabricating the die and the blank in order to obtain a physical product.
6. Start the test after the die and the blank are properly fabricated.
7. Secure the data during the experimental process and then use the optical microscope to measure till obtaining final outline dimensions.
8. Compare the experiment result and the value analysis result. Check if the results of both are identical and then analyze the error level.
9. Compare the experiment and the simulation results in order to confirm if the theory used for this research is correct.

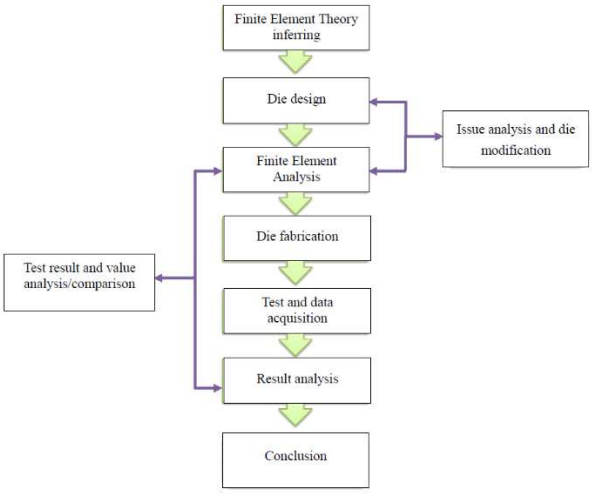

Fig 2. Research Step Flow Chart

3. Experiment Verification and Analysis

3.1 Torque comparison for test and simulation

Indicated in Figs. 3 and 4 are the torque comparative diagrams relating to the experiment and the simulation. To determine the friction factors that should be set for the simulation, assume that the friction factors are set as 0.2 and 0.3 for carrying out the comparative verification with the experiment values. As indicated in the figure, when setting the friction factor at 0.3 (i.e. m=0.3), the torsional curve resolved from the simulation is closer to the experiment curve trend. Therefore, the friction factor of m=0.3 is selected for the value simulation analysis described in this article in order to analyze the screw thread forming process for micro-type circular rods.

3.2 Tooth shape comparison for the experiment and the simulation

To justify the accuracy between the experiment and the simulation being conducted during the research, the optical microscope is used to measure the difference in tooth angle and tooth height of the product to study the difference of the models being used during the experiment the simulation. Indicated in Fig. 5 is the comparison of tooth shape required for the experiment and the simulation. As indicated in the figure, the tooth angle measured for the simulated M2x0.25 is 60.431° and that measured during the test is 60.552°, presenting 0.2% of error. The height difference for the simulated tooth is 0.06mm and that measured during the test is 0.065mm, presenting 7.629% of error. The tooth angle measured for the simulated M2x04 is 60.987° and that measured during the test is 60.421°, presenting 0.937% of error. The height difference measured for the simulated tooth is 0.039mm and that measured during the test is 0.036mm, presenting 8.333% of error.

4. Result and Discussions

4.1 Forming process

During the simulation process, the pitch fluctuation values are 0.25mm and 0.4mm respectively; the fluctuation values of the friction factors are 0.1, 0.2, 0.3, 0.5 and 0.7 respectively; and the fluctuation value of the circular rod diameters are 1.9mm, 1.94mm and 2mm respectively. Indicated in Fig. 6 is the die and blank position layout for the screw die, and indicated in Fig. 7 is the 5-stage geometric forming diagram relating to the micro-type circular rod screw thread forming.

4.2 Comparison of torque

Indicated from Fig. 8 to Fig. 10 are the relationship between the screw die torque and the pitch stroke before and after the scale factor is modified. From these figures, the screw die torque will increase rapidly soon as contacting the micro-type circular rod. The screw die torque begins to increase soon as the screw die pushes against the parts during the downward rotating process. The results indicate that the torque of the screw die increases along with the enlarging of the pitch.

Indicated in Fig. 11 to Fig. 16 is the relationship between the friction factors and the stroke of screw die torque. The aforesaid figures indicated that when the friction factors are changed during the screw thread machining process for the micro-type circular rod, the torque of the screw die will increase along with the soaring of the friction factors.

4.3 Difference of stress and strain

Figs. 17 and 18 explain the relationship between the pitch and the maximum principal stress in which, the maximum principal stress is presented in the micro-type circular rod thread forming area and such stress is expressed by MPa as the measuring unit. As indicated in the figures, the max. principal stress tends to grow along with the enlarging of the pitch. Indicated in Fig. 17 is the 0.25mm pitch that will be used to execute the thread tapping for the circular rods with the outer diameter being set as Ø1.9mm, Ø1.94mm and Ø2mm, respectively. When the diameter of the modified circular rod becomes 1.9mm, the max. principal stress is shown as 22,800 MPa; when the diameter of the circular rod becomes 1.94mm, the max. principal stress is shown as 23,100 MPa; and when the diameter of the circular rod becomes 2mm, the max. principal stress is shown as 30,100 MPa. Indicated in Fig. 18 is the 0.4mm pitch that will be used to execute the thread tapping for the circular rods with the outer diameter being set as Ø1.9mm, Ø1.94mm and Ø2mm, respectively. When the diameter of the modified circular rod becomes 1.9mm, the max. principal stress is shown as 21,000 MPa; when the diameter of the modified circular rod becomes 1.94mm, the max. principal stress is shown as 22,900 MPa; and when the diameter of the modified circular rod becomes 2mm, the max. principal stress is shown as 30,220 MPa.

Fig. 19 to Fig. 21 explain the relationship between the friction factor and the max. principal stress in which the max. principal stress is presented in the micro-type circular rod thread forming area and such stress is expressed by MPa as the measuring unit. As indicated in the aforesaid figures, the max. principal stress tends to grow along with the increase of friction factors.

Figs. 22 and 23 explain the relationship between the pitch and the maximum principal strain in which, the max. principal strain is presented in the micro-type circular rod thread forming area and such strain is expressed by “mm/mm” as the measuring unit. As indicated in the figures, the max. principal strain tends to grow along with the enlarging of the pitch. Indicated in

Fig. 22 is the 0.25mm pitch that will be used to execute the thread tapping for the circular rods with the outer diameter being set as Ø1.9mm, Ø1.94mm and Ø2mm, respectively. When the diameter of the modified circular rod becomes 1.9mm, the max. principal strain is shown as 0.672; when the diameter of the circular rod becomes 1.94mm, the max. principal strain is shown as 0.725; and when the diameter of the circular rod becomes 2mm, the max. principal strain is shown as 0.964. Indicated in Fig. 23 is the 0.4mm pitch that will be used to execute the thread tapping for the circular rods with the outer diameter being set as Ø1.9mm, Ø1.94mm and Ø2mm respectively. When the diameter of the modified circular rod becomes 1.9mm, the max. principal strain is shown as 0.861; when the diameter of the modified circular rod becomes 1.94mm, the max. principal strain increases as 0.972; and when the diameter of the modified circular rod becomes 2mm, the max. principal strain changes to 1.45.

Fig. 24 to Fig. 26 explain the relationship between the friction factor and the max. principal strain. As indicated in the aforesaid figures, the max. principal strain tends to grow along with the increase of friction factors.

5. Conclusions

This article uses the SUS304 stainless steel circular rod as the testing material, with the die fabricated and the thread tapping mechanism designed to complete the experiment for the entire process. For this purpose, two kinds of pitches are selected to compare the influence of diameter and friction factor to the product during the analysis process conducted for three pieces of circular rods being fabricated into different dimensions. Further, the optical microscope is also used to observe the tooth shape supported with the finite element analysis so that the screw thread forming process could be accurately analyzed for the micro-type circular rods. Through the finite element simulation and the comparison of traditional and micro-type before and after the modification indicated that the max. principal stress tends to grow along with the increase of the pitch. However, the visible difference has not been observed in the max. principal stress before and after the modification. Meanwhile, the torsional value of the screw thread machining required for the circular rod tends to grow along with the enlarging of the rod's outer diameter. As the friction factors are changing during the micro-type circular rod screw thread machining process, the torque and the stress and the strain of the screw die will grow along with the increase of friction factors.

Declarations

a. Funding :The financial support of this research by Ministry of Science and Technology in Taiwan, under the projects No. Most-109-2221-E-194 -050 and Most-108-2218-E-194 -013 are greatly appreciated.

b. Conflicts of interest/Competing interests (include appropriate disclosures): There isn't any conflicts of interest/competing interests for anyone or parties.

c. Availability of data and material (data transparency):All of the data and materials in this manuscript are analyzed and studied by ourselves.

d. Code availability (software application or custom code): All of the simulation results are analyzed by applying software with legal liscense.

e. Ethics approval (include appropriate approvals or waivers): All research results have nothing to do with ethics and do not violate any academic ethics and other issues.

f. Consent to participate (include appropriate statements):All authors agree the consent to participate of the Journal’s regulations.

g. Consent for publication (include appropriate statements) :All authors agree and follow the consent for publication of the Journal’s regulations.

h. Authors' contributions: There are three authors including Tsung-Chia Chen(TC Chen), Hao-Wei Ting(HW Ting), Cheng-Chi Wang(CC Wang). Chen and Ting conceived of the presented idea and developed the theory and performed the computations of simulation. Ting and Wang verified the analytical methods by experiments. Wang supervised the findings of this work. All authors discussed the results and contributed to the final manuscript.

References

1. Makinouchi, and M. Kawka, “Process simulation in sheet metal forming,” Journal of Materials Processing Technology, Vol.46, pp.291-307, 1994.
2. U. Engel, and R. Eckstein, “Microforming-From Basic Reaearch to Its Realization,” Journal of Materials Processing Technology, Vol.125-126, pp.35-44, 2002.
3. L. Peng, X. Lai, H. J. Lee, J. H. Song, and J. Ni, “Friction behavior modeling and analysis in micro/meso scale metal forming process,” Materials and Design, vol. 31, no. 4, pp. 1953-1961, 2010.
4. R. Chiba, “Reliability analysis of forming limits of anisotropic metal sheets with uncertain material properties,” Computational Materials Science, vol. 69, pp. 113-120, 2013.
5. J. P. Domblesky, and F. Feng, “A parametric study of process parameters in external thread rolling,” Journal of Materials Processing Technology, vol. 121, no. 2-3, pp. 341-349, 2002.
6. U. Engel, and R. Eckstein, “Microforming-from basic research to its realization,” Journal of Materials Processing Technology, vol. 125–126,

pp. 35-44, 2002.

7. Z. Pater, A. Gontarz, and W. Weroñski, “New method of thread rolling,” Journal of Materials Processing Technology, vol. 153-154, pp. 722-728, 2004.
8. A. Gontarz, Z. Pater, and W. Weroñski, “Head forging aspects of new forming process of screw spike,” Journal of Materials Processing Technology, vol. 153-154, pp. 736-740, 2004.
9. Y. C. Kao, H. Y. Cheng, and C. H. She, “Development of an integrated CAD/CAE/CAM system on taper-tipped thread-rolling die-plates,” Journal of Materials Processing Technology, vol. 177, no. 1-3, pp. 98-103, 2006.
10. Kai-neng Huang, 2011, Study on Forging and Thread-rolling Processes of Magnesium Alloy Screws, National Sun Yat-sen University, Master Thesis.
11. Yung-Chin Li, 2014, Investigation of Tapping SUS 304 Using Micro-Taps, Ta Hwa University of Science and Technology, Master Thesis.
12. S. Pawar, and S. S. Joshi, “Experimental analysis of axial and torsional vibrations assisted tapping of titanium alloy,” Journal of Manufacturing Processes, vol. 22, pp. 7-20, 2016.
13. E. Oezkaya, and D. Biermann, “Segmented and mathematical model for 3D FEM tapping simulation to predict the relative torque before tool production,” International Journal of Mechanical Sciences, vol. 128-129, pp. 695-708, 2017.
14. Chern, G.-L., Wu, Y.-J. E. & Liu, S.-F., Development of a micro-punching machine and study on the influence of vibration machining in micro-EDM. J. Mats. Proc. Tech., 180, 102-109, 2006.

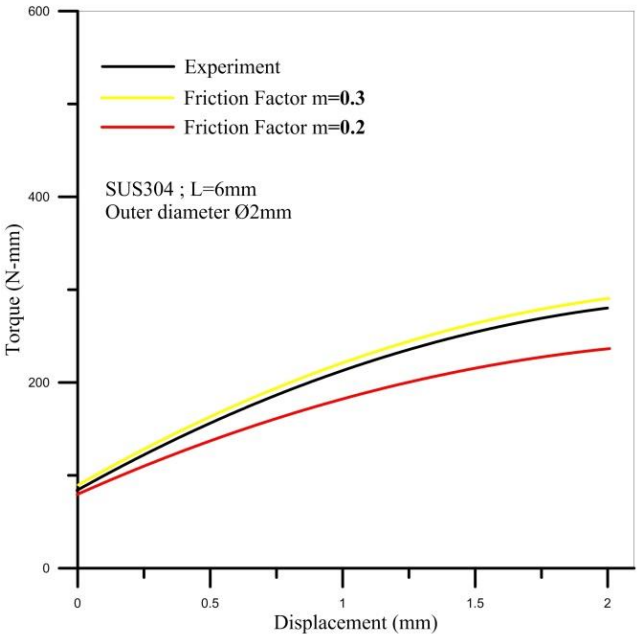

Fig. 3. Torque Comparative Relationship Diagram for Experiment and Simulation (M2x0.25)

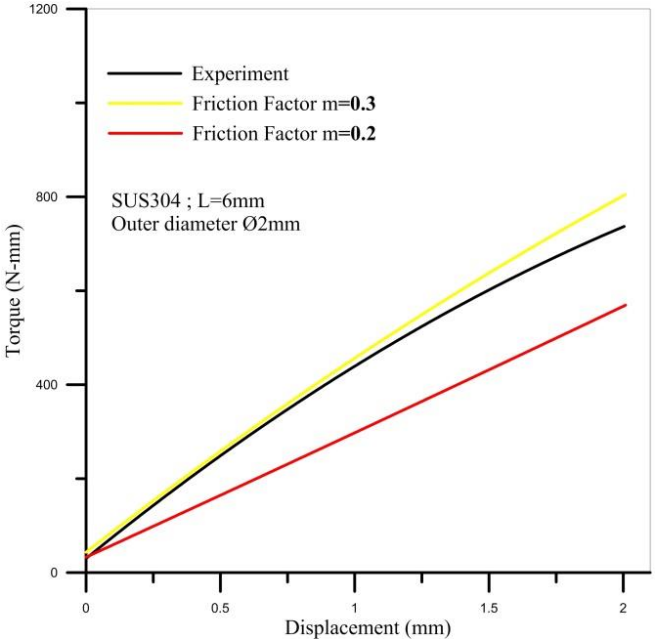

Fig. 4. Torque Comparative Relationship Diagram for Experiment and Simulation (M2x0.4)

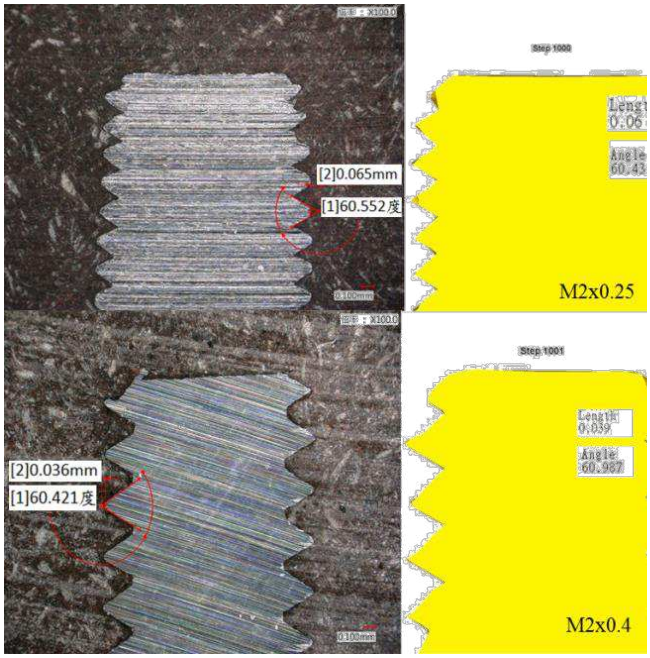

Fig. 5. Thread Shape Comparative Relationship Diagram for Experiment and Simulation

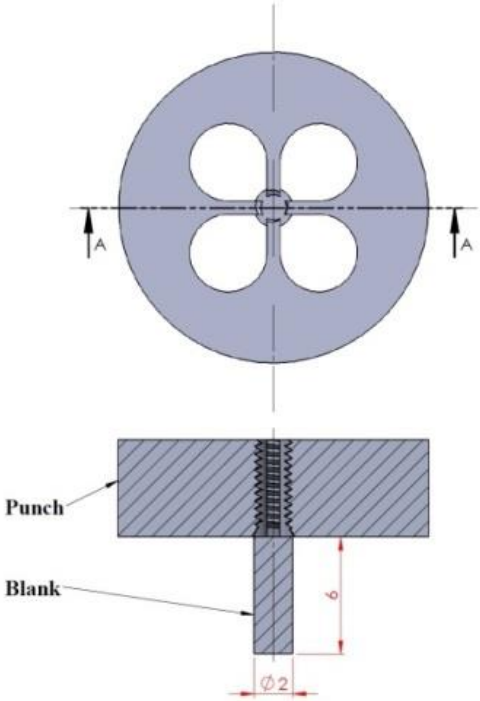

Fig. 6. Screw Die and Blank Position Schematic

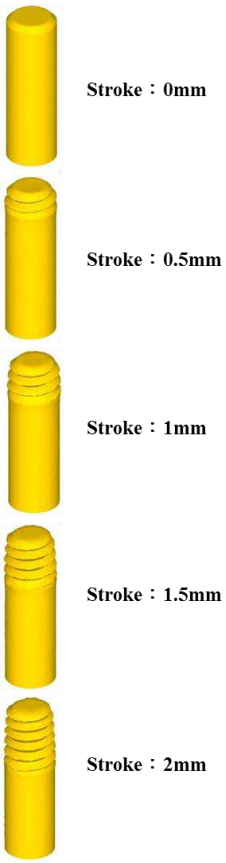

Fig. 7. Geometric Forming Diagram

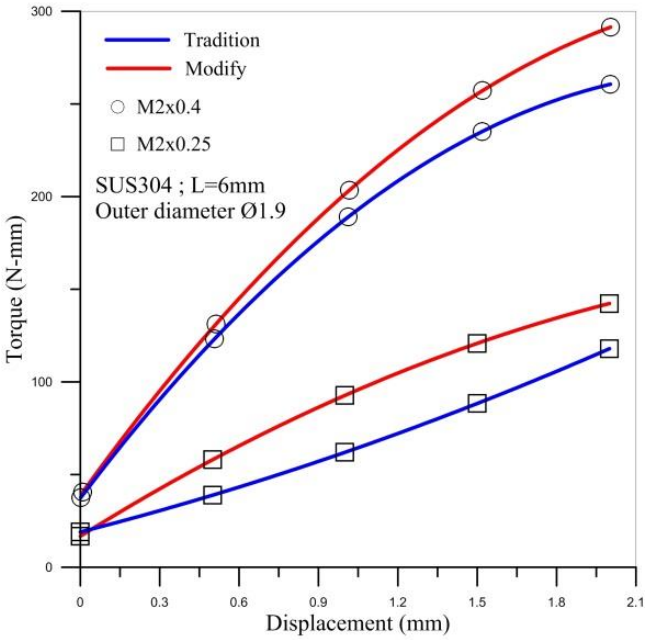

Fig. 8. Relationship between Torque and Pitch Stroke (for Ø1.9mm)

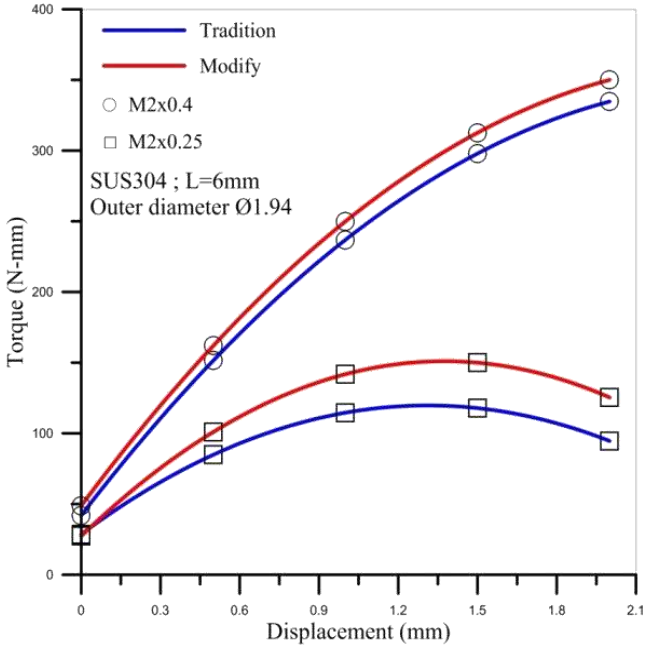

Fig. 9. Relationship between Torque and Pitch Stroke (for Ø1.94mm)

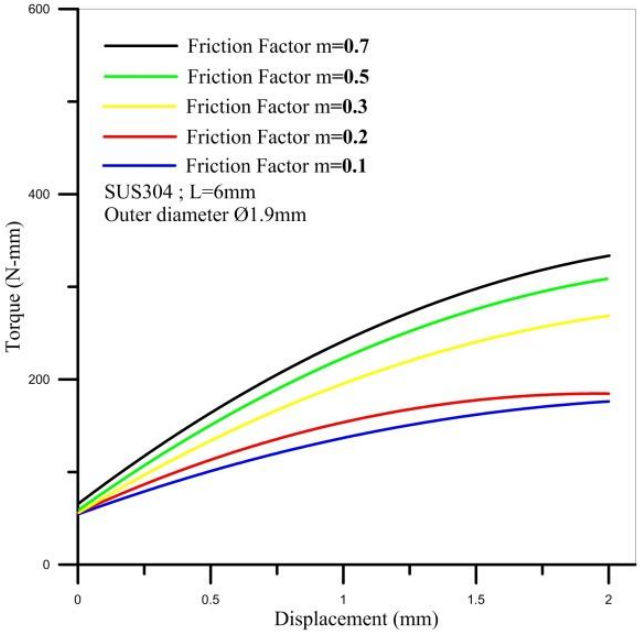

Fig.11. Relationship between Friction Factor and Torque Stroke (for M2x0.25)

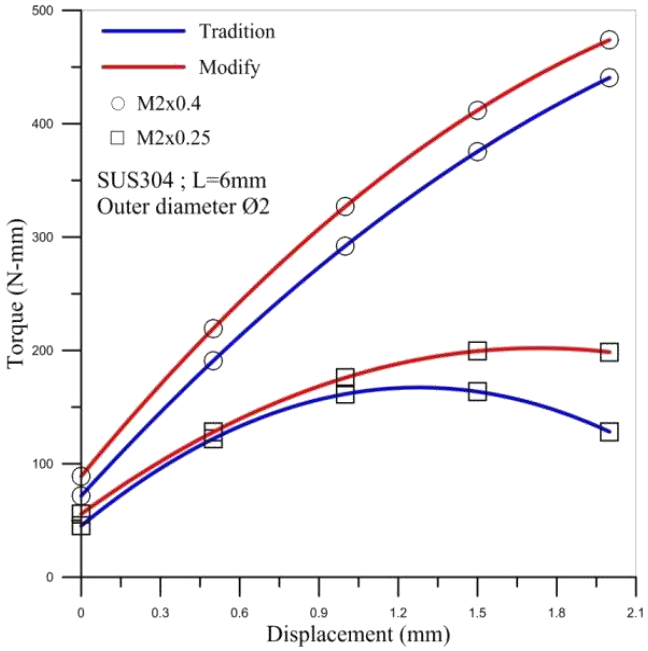

Fig. 10. Relationship between Torque and Pitch Stroke (for Ø2mm)

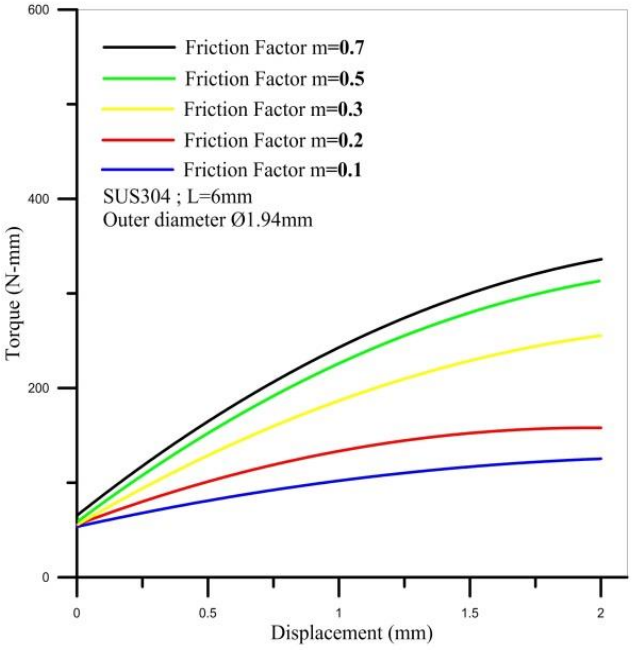

Fig. 12. Relationship between Friction Factor and Torque Stroke (for M2x0.25)

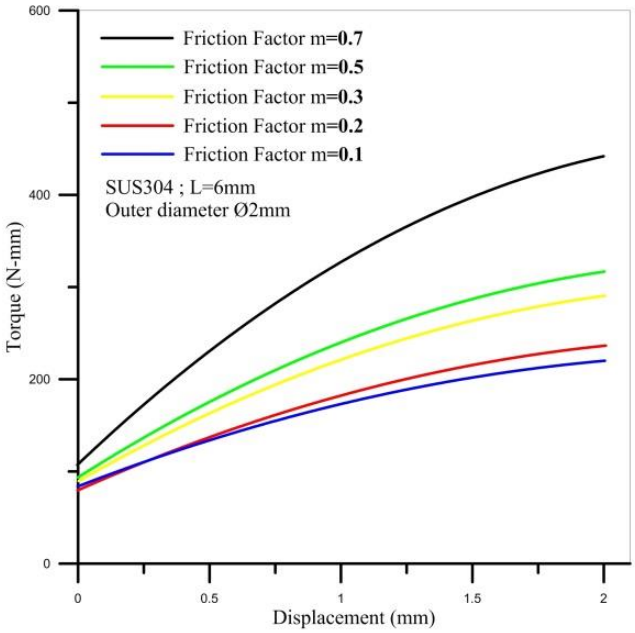

Fig. 13. Relationship between Friction Factor and Torque Stroke (for M2x0.25)

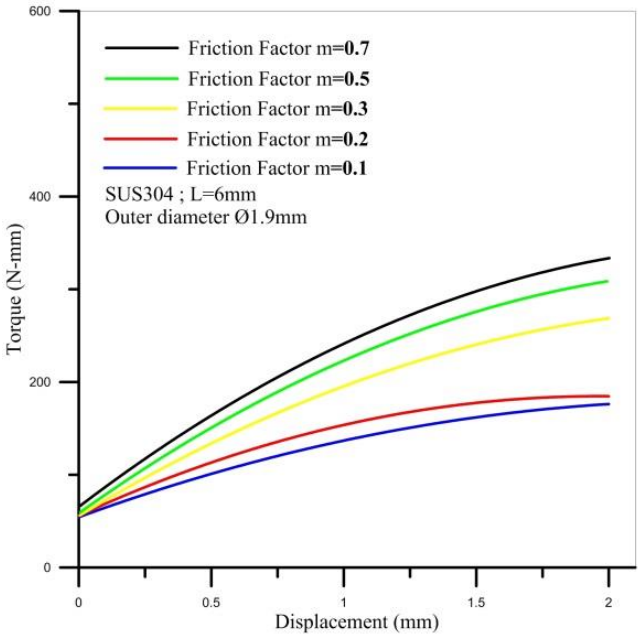

Fig. 14. Relationship between Friction Factor and Torque Stroke (for M2x0.4)

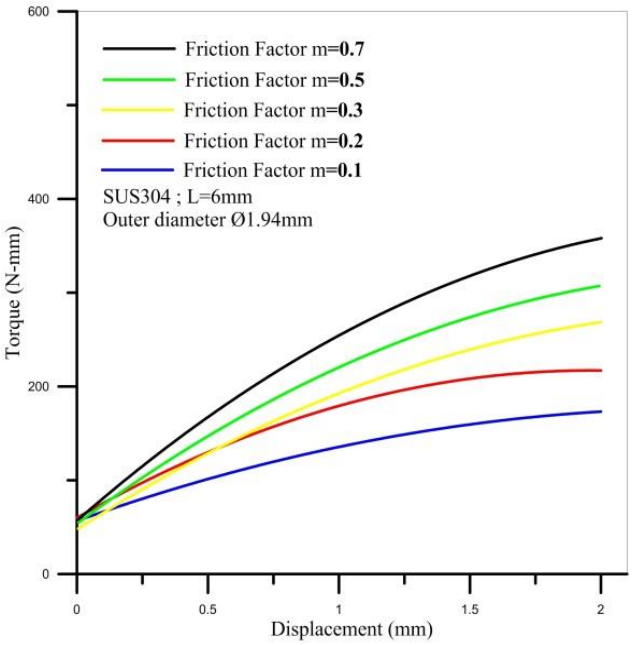

Fig. 15. Relationship between Friction Factor and Torque Stroke (for M2x0.4)

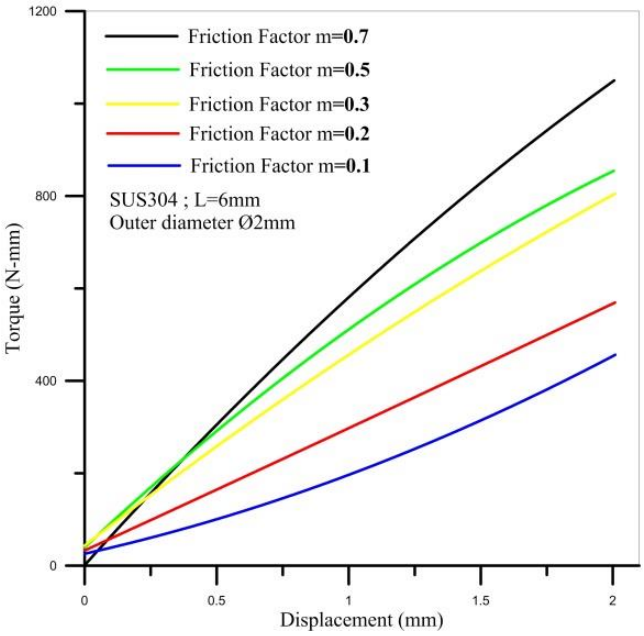

Fig. 16. Relationship between Friction Factor and Torque Stroke (for M2x0.4)

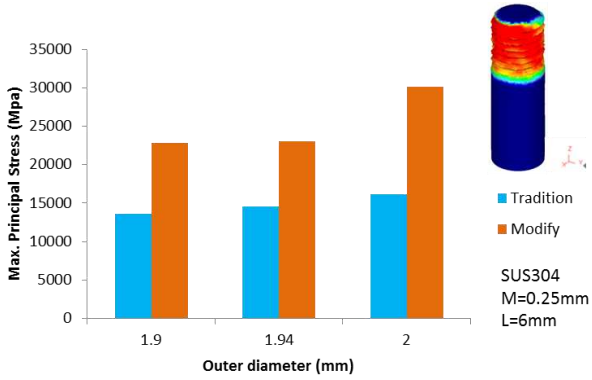

Fig. 17. Relationship between Pitch and Max. Principal Stress (for M2x0.25)

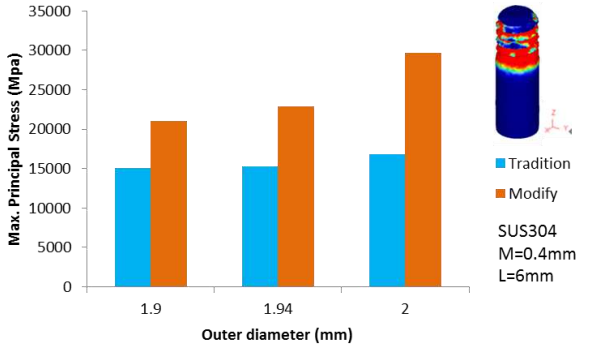

Fig. 18. Relationship between Pitch and Max. Principal Stress (for M2x0.4)

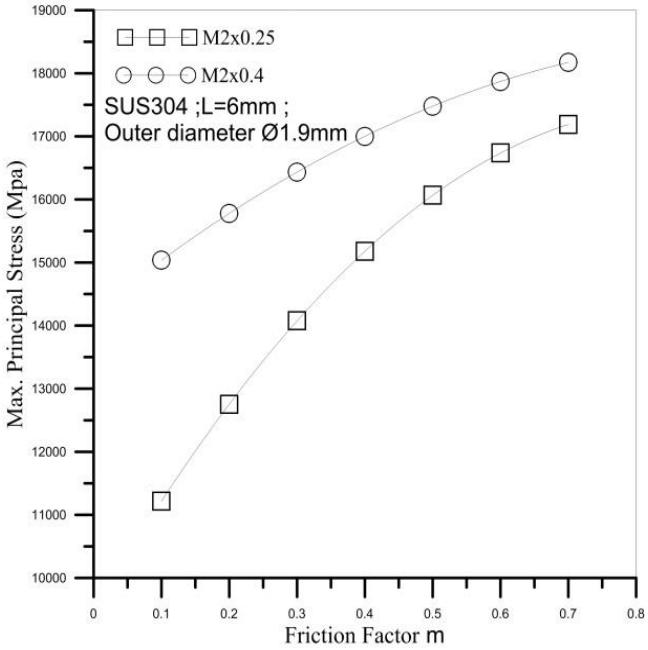

Fig. 19. Relationship between Friction Factor and Max. Principal Stress (for Ø1.9mm)

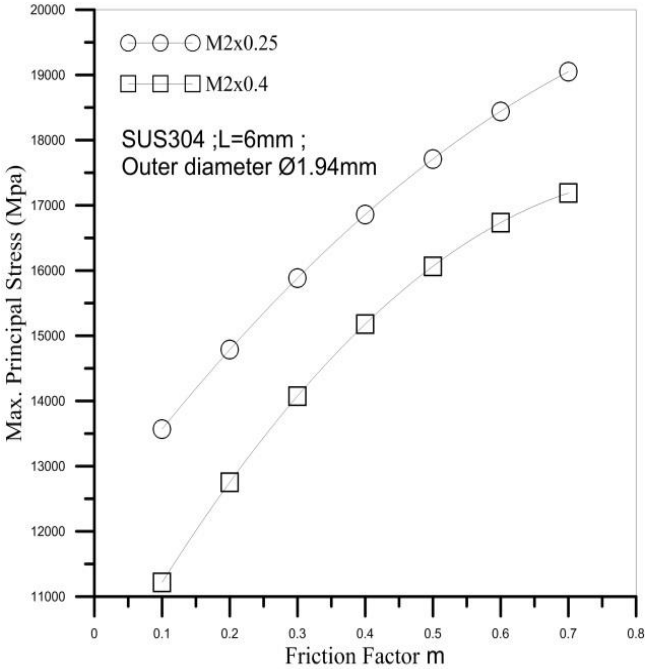

Fig. 20. Relationship between Friction Factor and Max. Principal Stress (for Ø1.94mm)

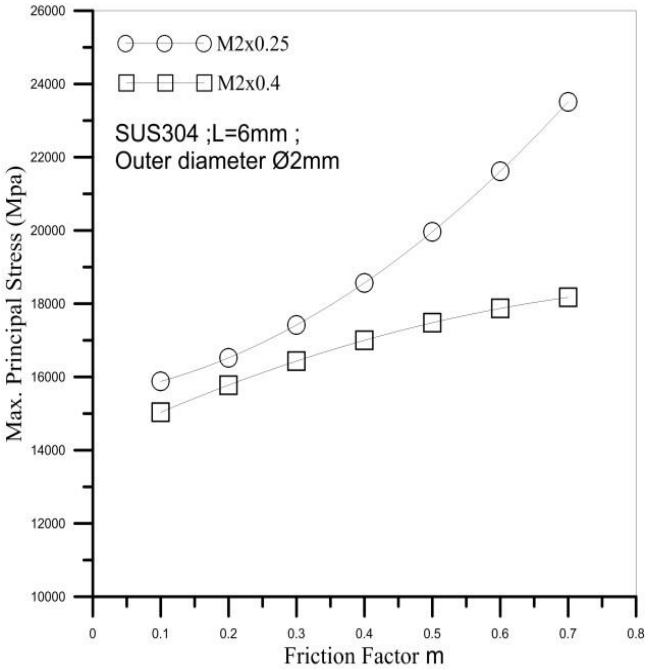

Fig. 21. Relationship between Friction Factor and Max. Principal Stress (for Ø2mm)

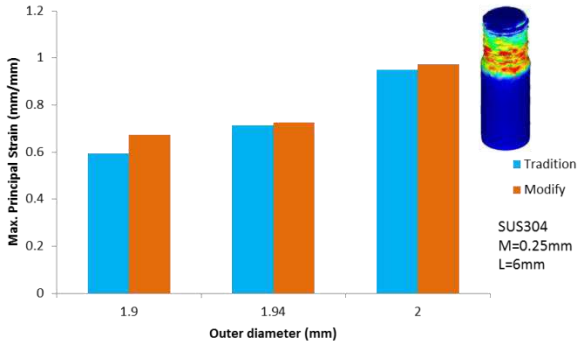

Fig. 22. Relationship between Pitch and Max. Principal Stress (for M2x0.25)

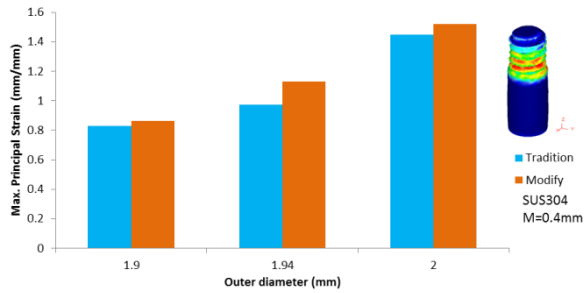

Fig. 23. Relationship between Pitch and Max. Principal Stress (for M2x0.4)

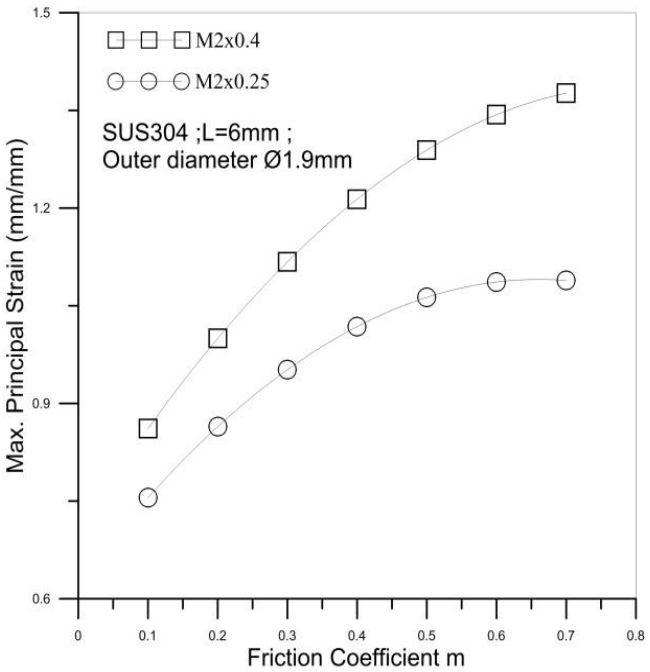

Fig. 24. Relationship between Friction Factor and Max. Principal Stress (for Ø1.9mm)

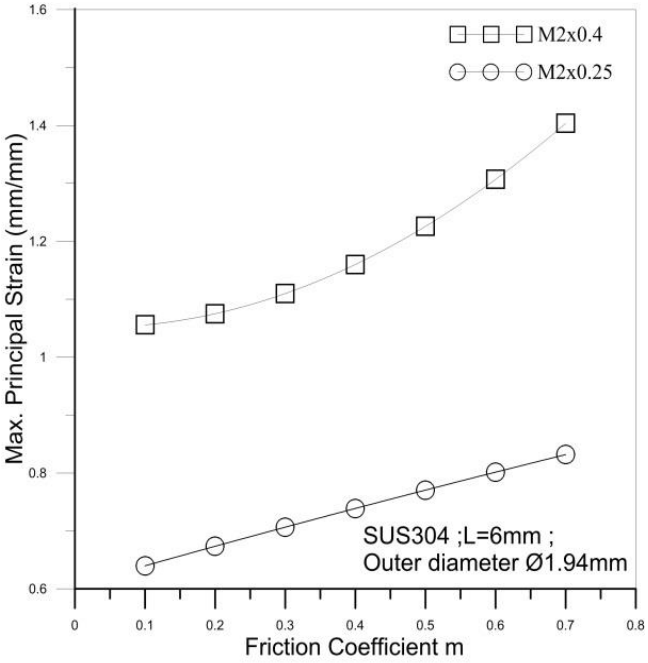

Fig. 25. Relationship between Friction Factor and Max. Principal Stress (for Ø1.94mm)

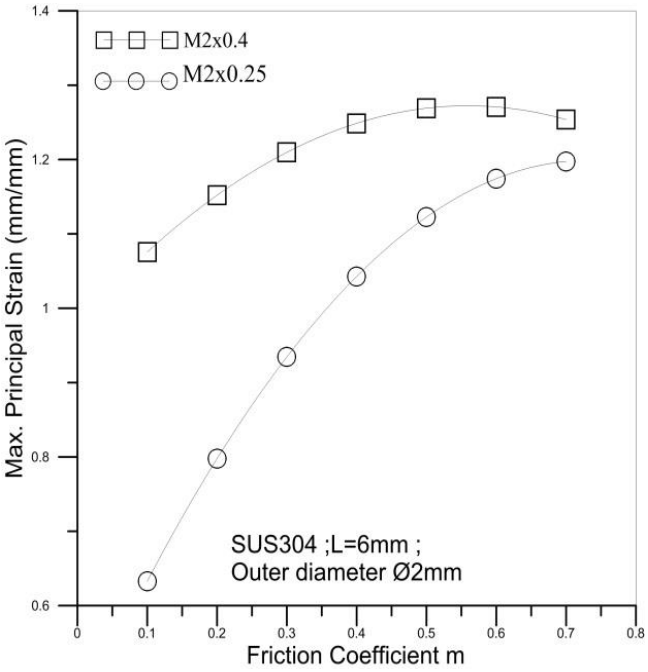

Fig. 26. Relationship between Friction Factor and Max. Principal Stress (for Ø2mm)

Figures

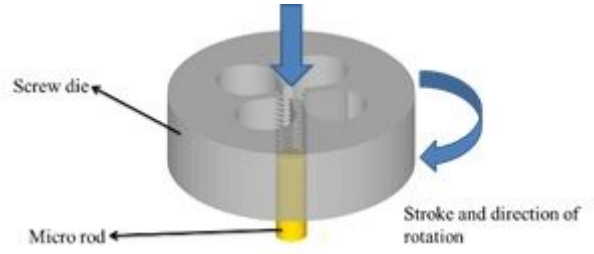

Figure 1

Action Method of Screw Die and Micro-type Circular Rod

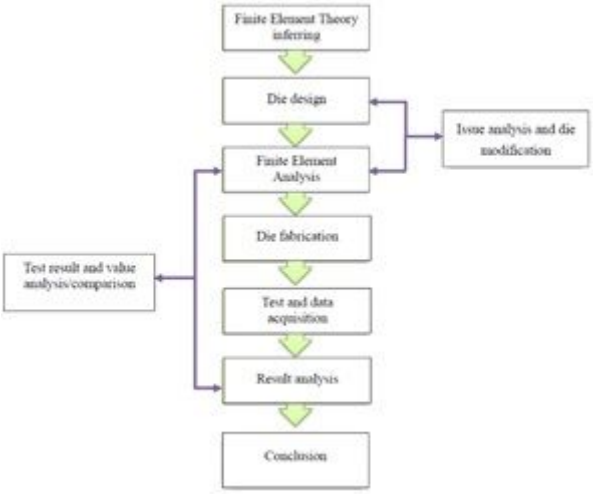

Figure 2

Research Step Flow Chart

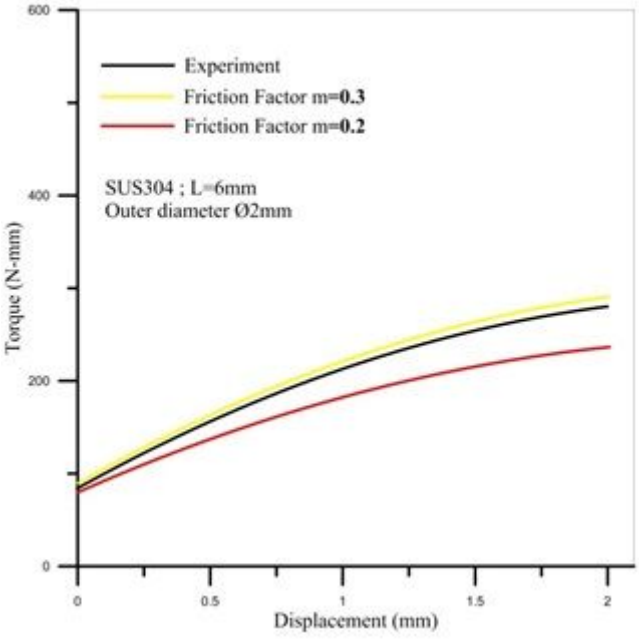

Figure 3

Torque Comparative Relationship Diagram for Experiment and Simulation (M2x0.25)

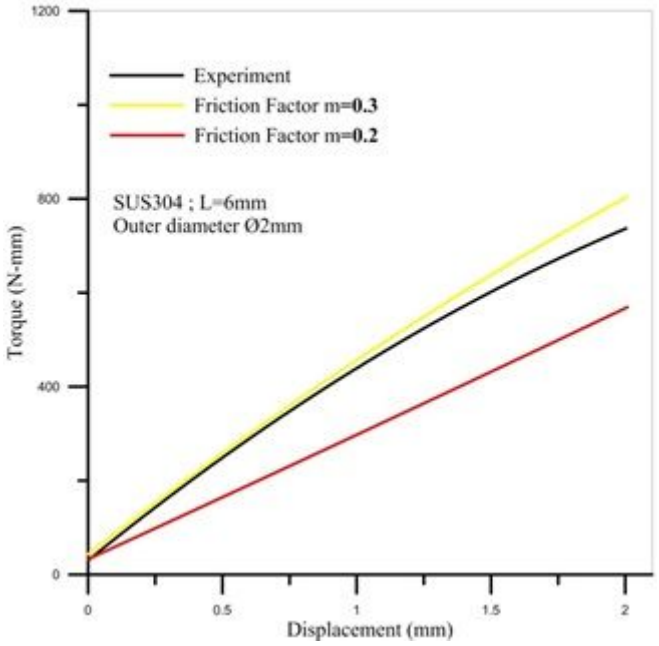

Figure 4

Torque Comparative Relationship Diagram for Experiment and Simulation (M2x0.4)

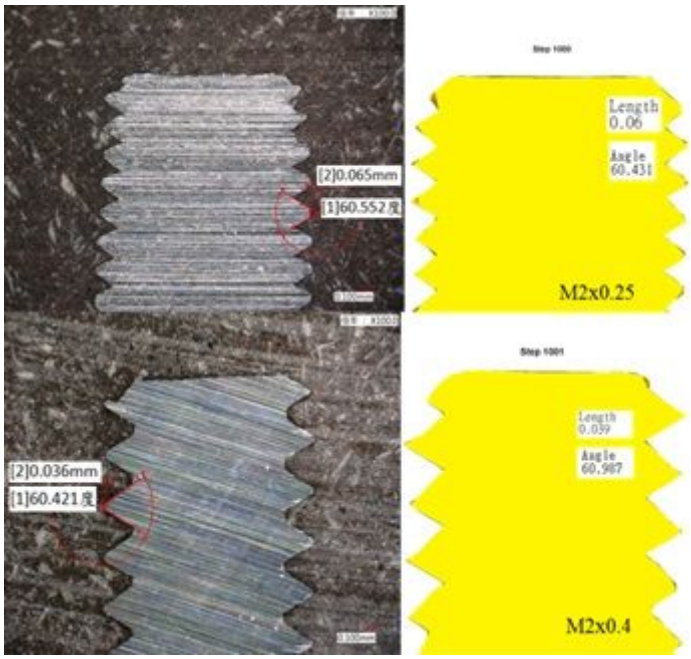

Figure 5

Thread Shape Comparative Relationship Diagram for Experiment and Simulation

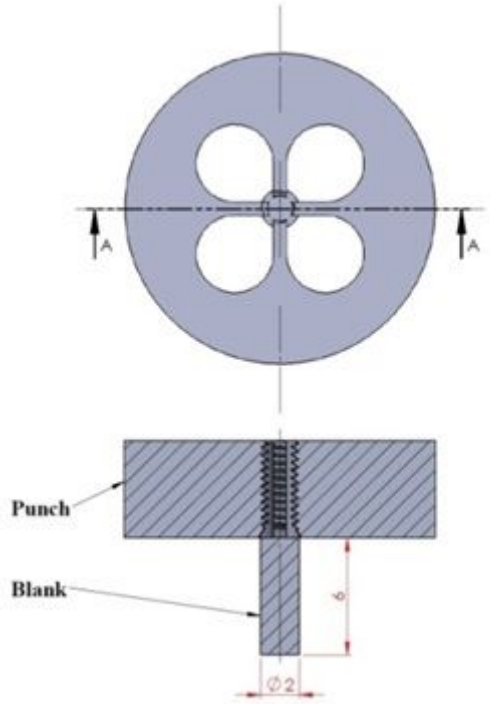

Figure 6

Screw Die and Blank Position Schematic

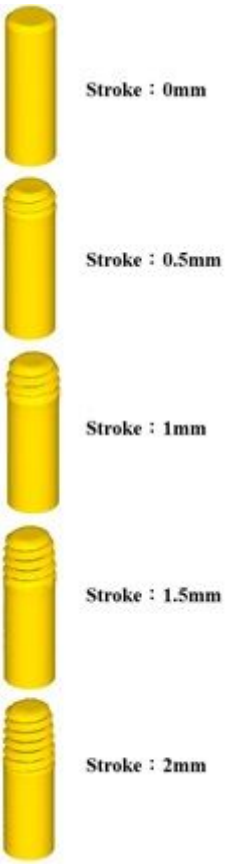

Figure 7

Geometric Forming Diagram

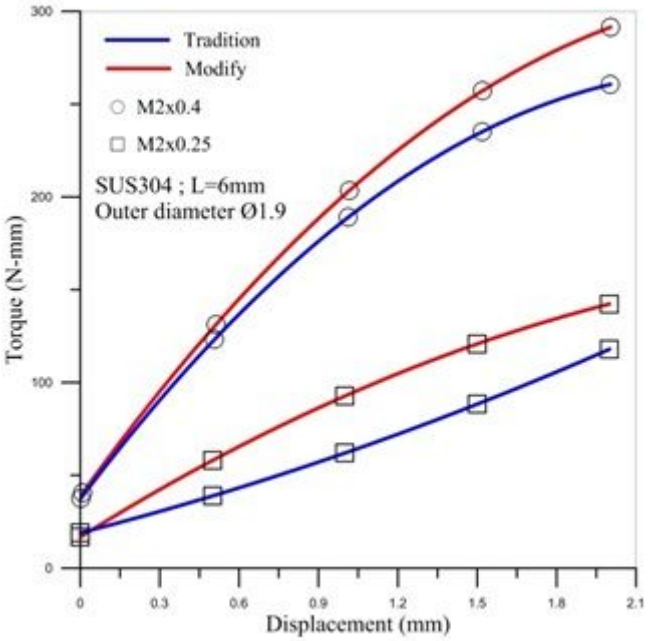

Figure 8

Relationship between Torque and Pitch Stroke (for Ø1.9mm)

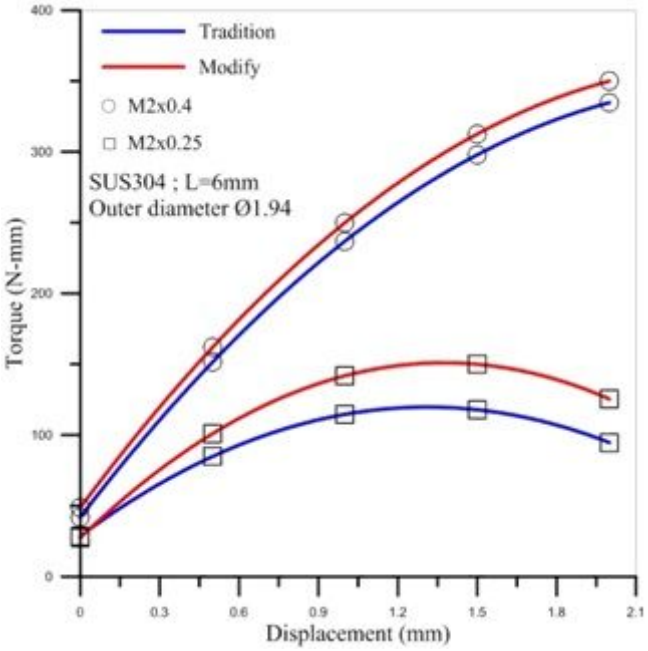

Figure 9

Relationship between Torque and Pitch Stroke (for Ø1.94mm)

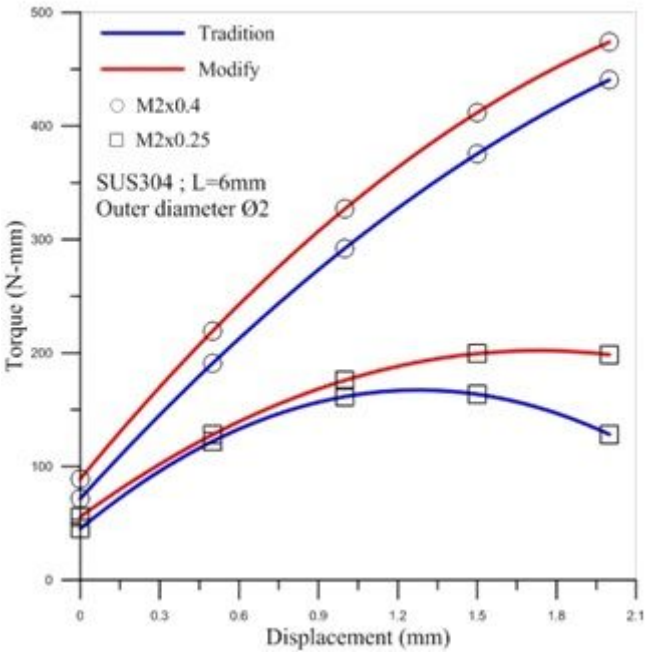

Figure 10

Relationship between Torque and Pitch Stroke (for Ø2mm)

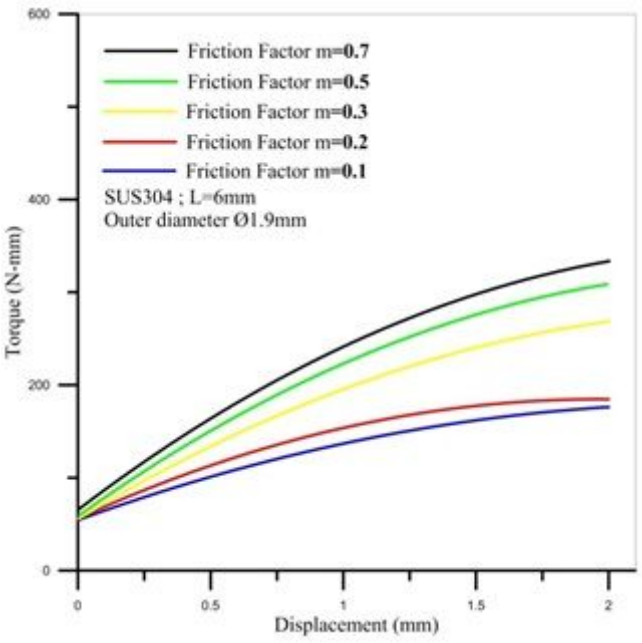

Figure 11

Relationship between Friction Factor and Torque Stroke (for M2x0.25)

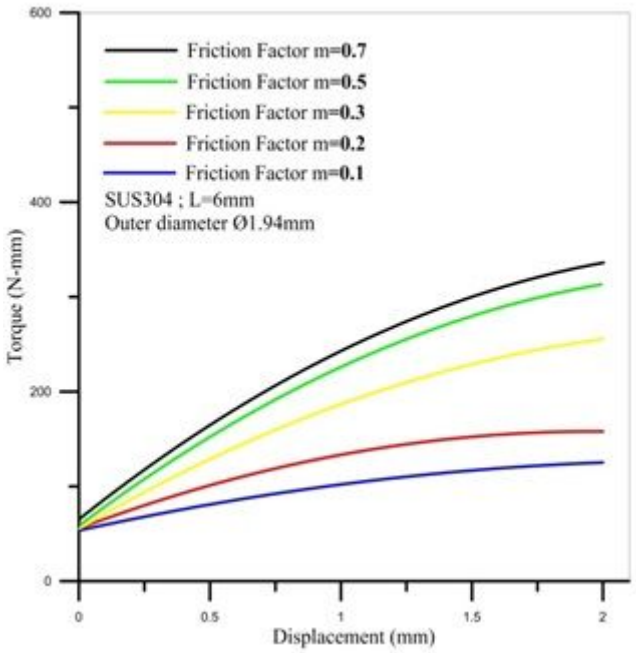

Figure 12

Relationship between Friction Factor and Torque Stroke (for M2x0.25)

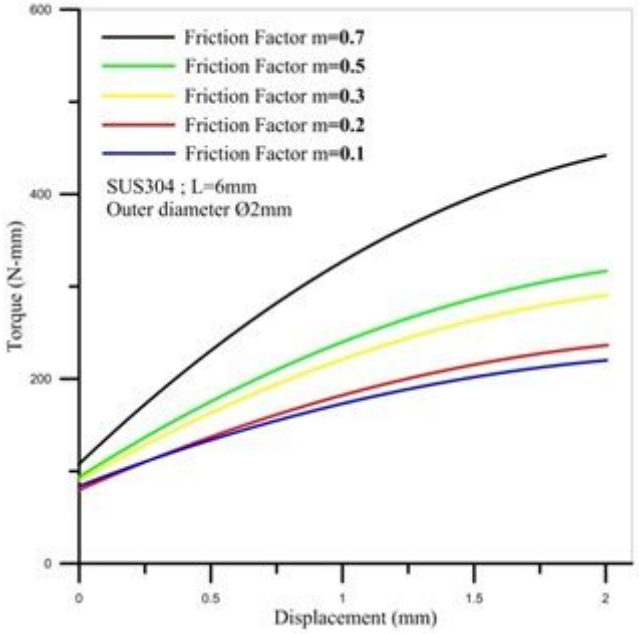

Figure 13

Relationship between Friction Factor and Torque Stroke (for M2x0.25)

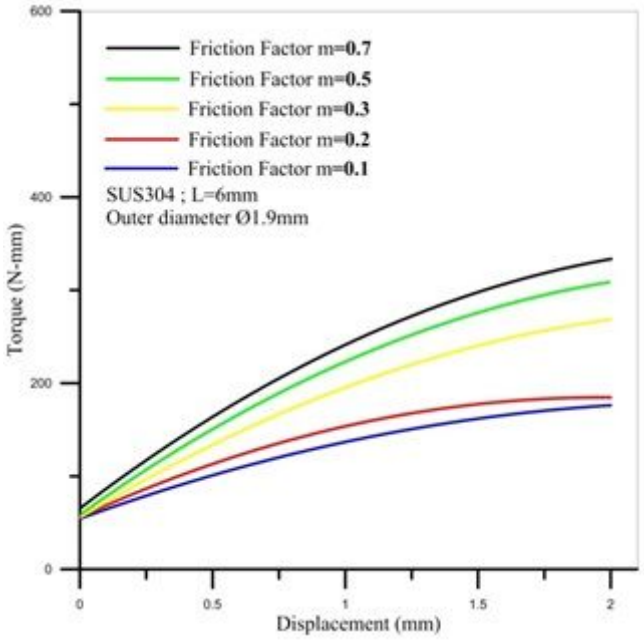

Figure 14

Relationship between Friction Factor and Torque Stroke (for M2x0.4)

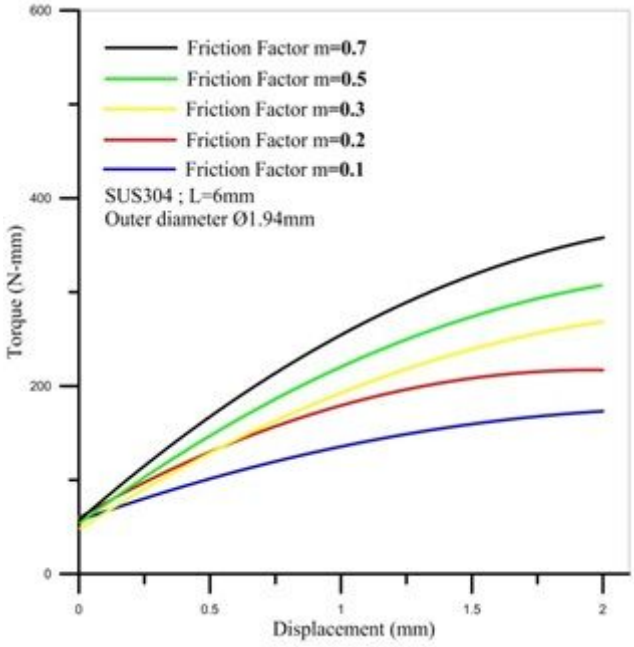

Figure 15

Relationship between Friction Factor and Torque Stroke (for M2x0.4)

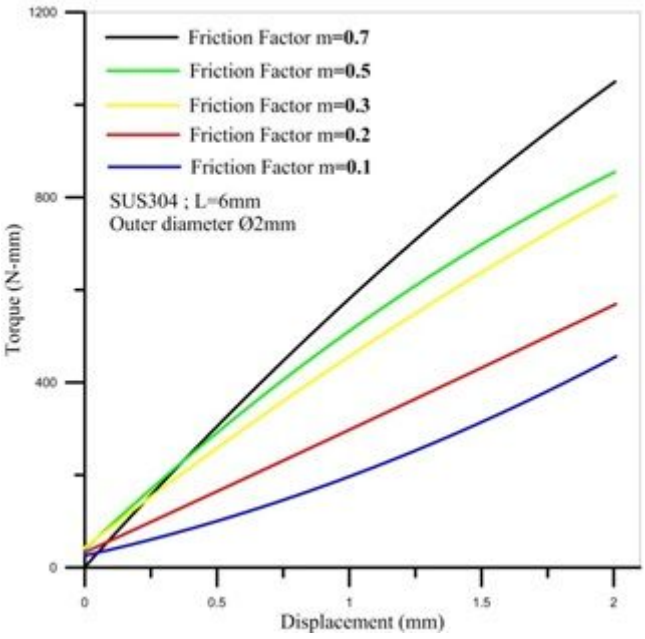

Figure 16

Relationship between Friction Factor and Torque Stroke (for M2x0.4)

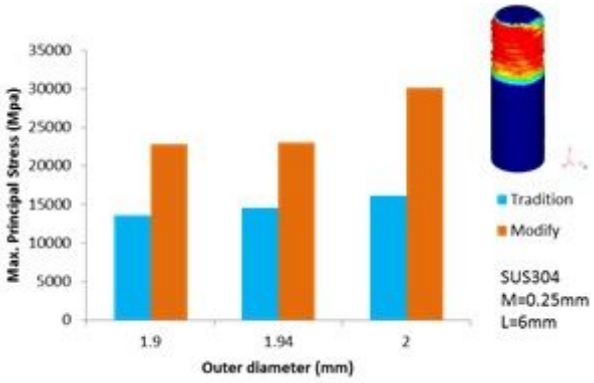

Figure 17

Relationship between Pitch and Max. Principal Stress (for M2x0.25)

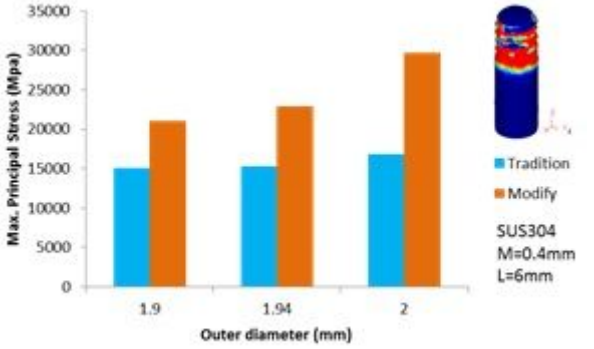

Figure 18

Relationship between Pitch and Max. Principal Stress (for M2x0.4)

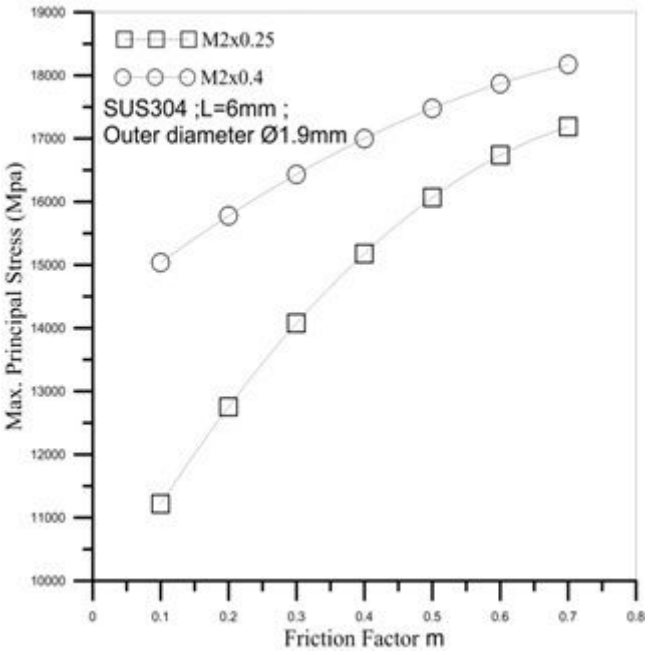

Figure 19

Relationship between Friction Factor and Max. Principal Stress (for Ø1.9mm)

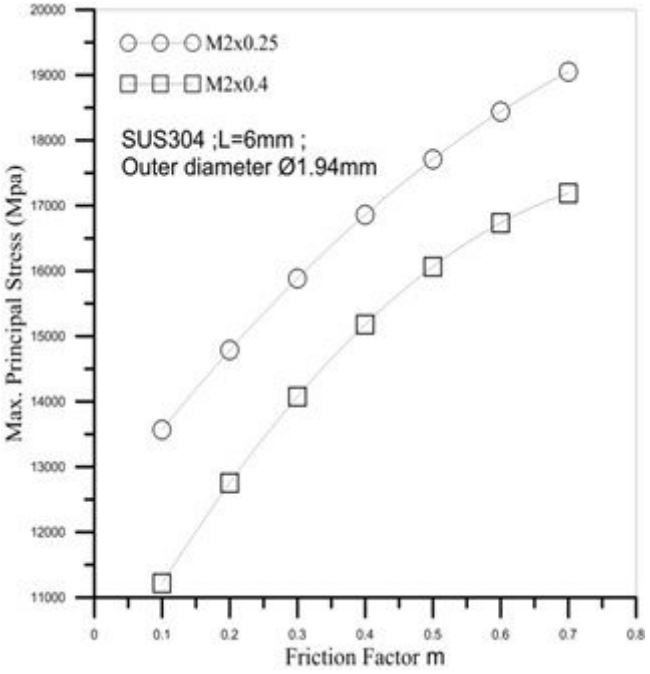

Figure 20

Relationship between Friction Factor and Max. Principal Stress (for Ø1.94mm)

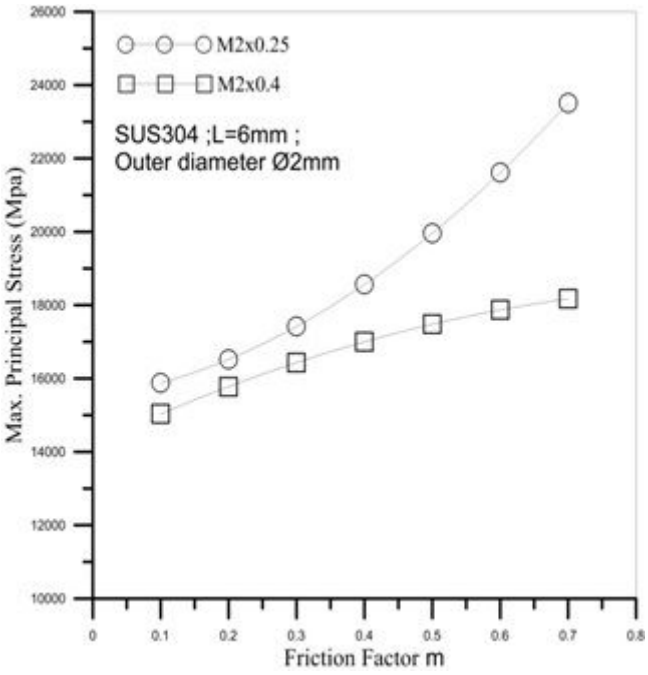

Figure 21

Relationship between Friction Factor and Max. Principal Stress (for Ø2mm)

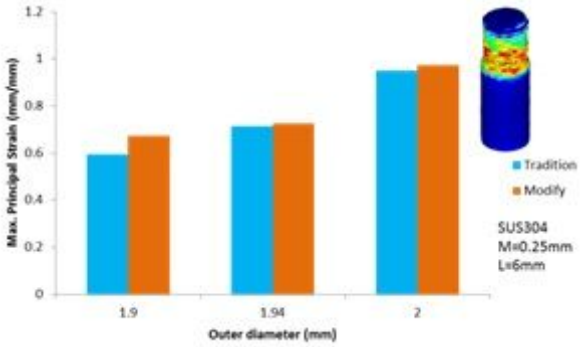

Figure 22

Relationship between Pitch and Max. Principal Stress (for M2x0.25)

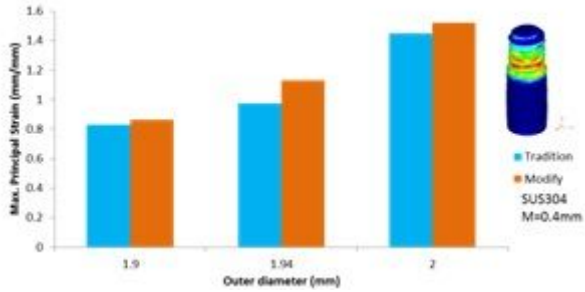

Figure 23

Relationship between Pitch and Max. Principal Stress (for M2x0.4)

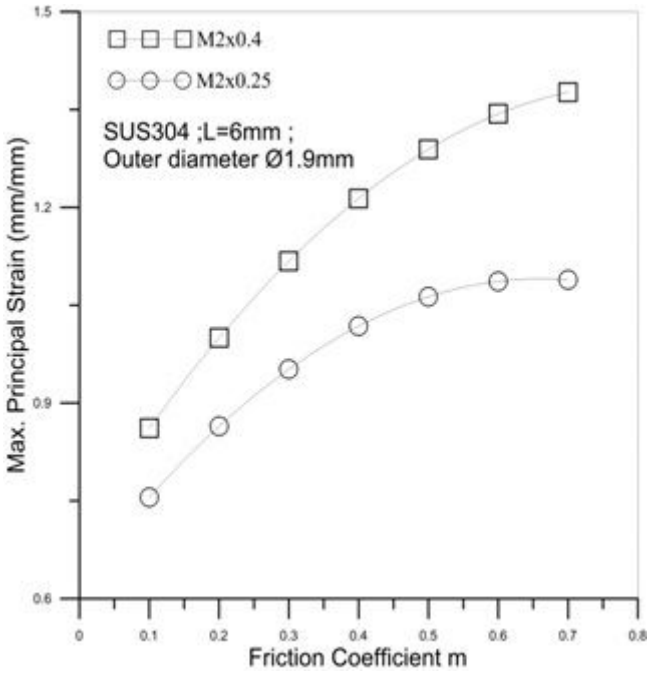

Figure 24

Relationship between Friction Factor and Max. Principal Stress (for Ø1.9mm)

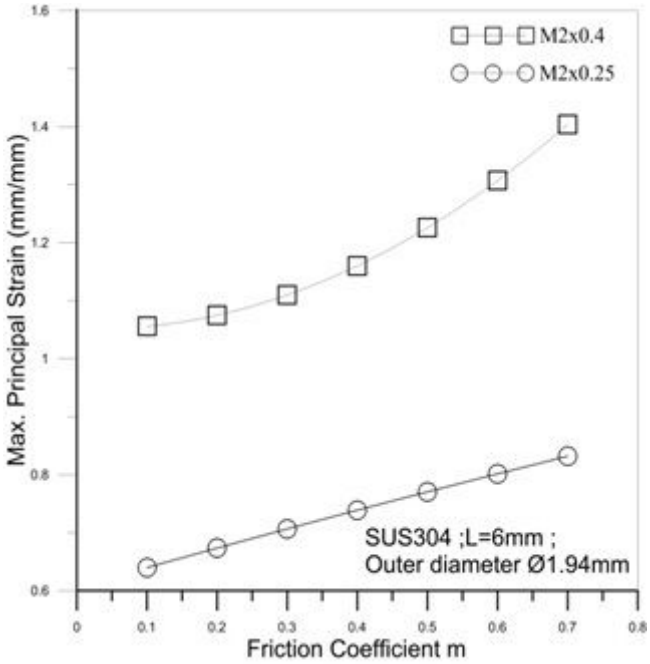

Figure 25

Relationship between Friction Factor and Max. Principal Stress (for Ø1.94mm)

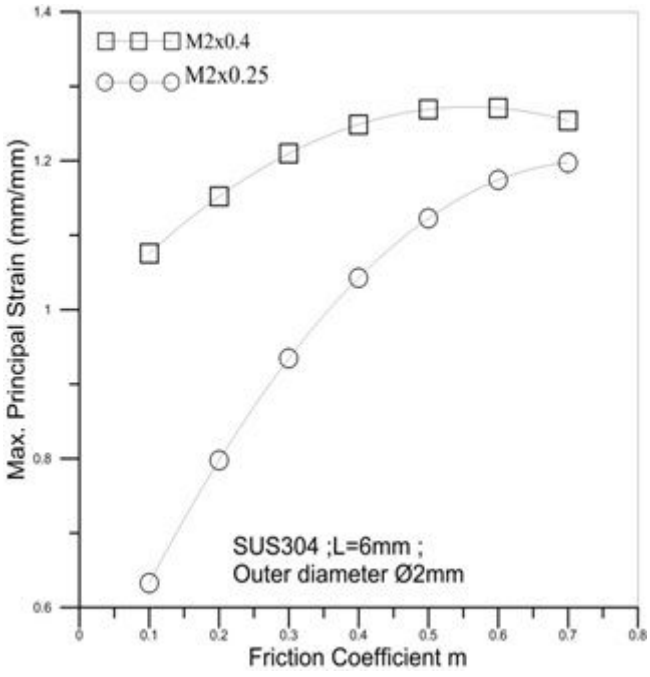

Figure 26

Relationship between Friction Factor and Max. Principal Stress (for Ø2mm)